PROCEEDINGS OF SCIENCE

Prospects for SUSY discovery after the LHC Run 1

Emanuele Bagnaschi*

Member of the MasterCode *collaboration*†
DESY, Notkestraße 85, D-22607 Hamburg, Germany
E-mail: emanuele.bagnaschi@desy.de

In this proceeding we report the recent study by the MasterCode collaboration [1] where we have performed a frequentist likelihood analysis of the parameter space of the pMSSM10. The pMSSM10 is a phenomenological scenario of the MSSM defined by 10 input parameters, which we specify at the scale $M_{\rm SUSY} = \sqrt{m_{\tilde{t}_1} m_{\tilde{t}_2}}$. The multi-dimensional parameter space was sampled using the MultiNest algorithm, for a total of 1.2×10^9 evaluated points. Experimental searches from ATLAS and CMS for strongly-interacting sparticles (jets, leptons + E_T signatures) and for electroweakly-interacting particles are included. Moreover we also consider Higgs sector (light Higgs mass and production rates), B-physics and electroweak precision observables. Finally, the constraints coming from the Cold Dark Matter (CDM) relic density and from the direct detection experiments (XENON100 and LUX) are included, assuming that the lightest neutralino provides the main component of the CDM density. Our analysis points out that the pMSSM10 provides a better fit to the available data, being able to accommodate without tension the measured value of $(g-2)_\mu$ and the exclusion constraints from the LHC, than the CMSSM, NUHM1 and NUHM2. We find, for the best fit point, a $\chi^2 = 20.5$ with 18 degrees of freedom (d.o.f.), excluding Higgs rates. In comparison, in the CMSSM, NUHM1 and NUHM2 we have a $\chi^2/\text{d.o.f} = 32.8/24$, $31.1/23$ and $30.3/22$ respectively.

The European Physical Society Conference on High Energy Physics
22-29 July 2015
Vienna, Austria

*Speaker.
†http://mastercode.web.cern.ch/

PoS(EPS-HEP2015)183

1. Introduction

The negative results from SUSY searches during LHC Run 1 [2, 3] have started to constraint significantly SUSY models, especially those that are based on unification assumptions at some Grand Unified Theory (GUT) scale. Indeed, in these models (e.g. the CMSSM [4, 5, 6], NUHM1 [7] and NUHM2 [8]) unification imposes a correlation between the masses of colored sparticles, which are strongly constrained by the LHC, and the masses of electroweakly-interacting sparticles, whose bounds from direct experimental searches are much less severe. These relations make difficult to explain the discrepancy between the observed $(g-2)_\mu$ value and the SM prediction via the additional contribution from SUSY particles, since the electroweakly-interacting sparticles are bounded to be relatively heavy by the limits on squarks and gluinos. Therefore phenomenological models, whose SUSY parameters are instead given at a low energy scale and are not correlated by any theoretical assumptions, are becoming more and more appealing.

The complete, unconstrained, phenomenological MSSM (pMSSM*n* [9]) introduces a large number of new parameters and it is therefore difficult to study effectively. We have therefore focused our attention on a reduced version with just 10 independent parameters, the pMSSM10. Following the experimental observation of the absence of sizable Flavor Changing Neutral Current (FCNC) beyond the Standard Model (SM) ones, we have assumed that the soft SUSY-breaking masses for the first two generations of squarks are equal and that the same holds for the three generations of sleptons. Moreover, for simplicity, we also assume that the soft-SUSY breaking masses for the left and right sfermions are the same and that the values of the scalar trilinear couplings are the same for all the sparticles. Finally, all the parameters are assumed to be real and their input value are defined at the scale $M_{\rm SUSY} = \sqrt{m_{\tilde{t}_1} m_{\tilde{t}_2}}$. The resulting set of input parameters is shown in table 1.

2. The `MasterCode` framework

The `MasterCode` is a frequentist fitting framework written in C++, Python and Cython. It interfaces several different public and private codes that provide the theoretical predictions for the observables that enter the global χ^2 function. All codes are linked together using the SUSY Les Houches Accord (SLHA) [10] standard.

The sampling of the multi-dimensional parameter space is performed using the `MultiNest` algorithm [11, 12, 13]. For the study of the pMSSM10, a total of $\sim 1.2 \times 10^9$ samples of the parameter space were computed. However it is computationally impossible to check the consistency of all these points with all the available collider searches. To overcome this obstacle the SUSY searches are split into three categories. The first one includes those searches that constraint the production of colored sparticles. We use then the approach outlined in ref. [14] to build a look-up table that depends only on the gluino, squark ($m_{\tilde{q}_{1,2}}$ and $m_{\tilde{q}_3}$) and LSP masses. The second one contains searches that are relevant for the production of electroweakly-interacting particles, while the third one is dedicated to compressed stop spectra. For these last two categories, we use specialized algorithms validated using the `Atom` [15] and `Scorpion` [16] codes. In all cases, all the information from the latest ATLAS and CMS searches has been included. Besides collider searches, we also include the constraints coming from:

pMSSM10 input parameters
M_1, M_2, M_3
$m_{\tilde{q}_{1,2}}, m_{\tilde{q}_3}, m_{\tilde{l}}$
A
$M_A, \tan\beta, \mu$

Table 1: Input parameters for the pMSSM10 model. From the top to the bottom row: the gaugino mass parameters; the squark and slepton mass parameters, with the assumptions outlined in the text; the unified trilinear coupling; the pseudoscalar Higgs mass (M_A), the ratio of the vacuum expectation values of the two Higgs doublets ($\tan\beta$) and Higgsino mass parameter (μ).

- Electroweak precision observables (`FeynWZ` [17])
- Flavor observables (`SuFla` [18], `SuperISO` [19]).
- Cosmological and direct detection dark matter constraints. In detail, we consider the spin independent proton cross section (`SSARD` [20]) and the cold dark matter relic density (`micrOMEGAs` [21]).
- Higgs sector observables, specifically the light Higgs mass and the production rates (`FeynHiggs` [22, 23], `HiggsSignals` [24], `HiggsBounds` [25]).

In the list above, we have specified in parenthesis the code that the we use in each case for the corresponding theoretical prediction. To generate the MSSM spectrum we have used `SoftSUSY` [26], while `SDECAY` [27] was used to calculate the sparticle branching ratios. We refer the reader to ref. [1] for an extensive explanation of the implementation of all the different experimental constraints included in our analysis.

3. Results

In the following section we first describe the main features of our fit, from the characteristics of the best fit point to the mass spectrum, and then we point out the reach for SUSY discovery at the LHC run 2 and at a future e^+e^- collider. For a more detailed discussion of our results, we refer again the reader to ref. [1].

3.1 Best fit point

In fig. 1 we plot the mass spectrum for the best-fit point of our pMSSM10 scan. We observe the following salient characteristics:

- There is a near degeneracy between the $\tilde{\chi}_1^0$, $\tilde{\chi}_2^0$ and $\tilde{\chi}_1^\pm$. This is a general feature of our 68% CL region and it is due to the CDM relic density constraint. The overall mass scale is determined from below by the LEP and LHC constraints and from above by the experimentally observed $(g-2)_\mu$ value.
- The mass scale of the gluino is relatively high, around 2.5 TeV, because of LHC searches, though the precise value is poorly determined.

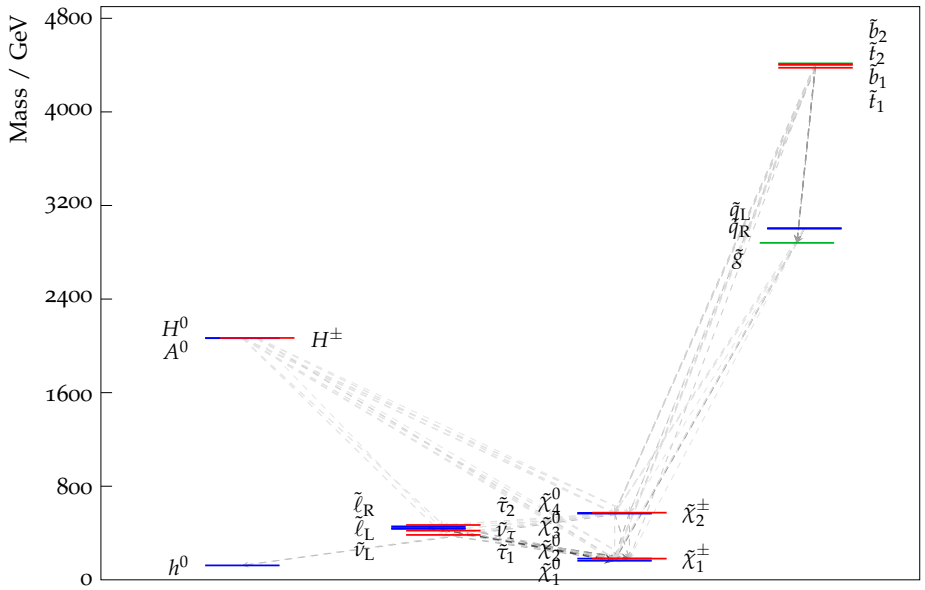

Figure 1: Mass spectrum for the best-fit point. The dominant decay channels are shown with dashed lines.

- There is a near degeneracy between the slepton masses due to our assumption of a unified value for the soft SUSY-breaking masses in the slepton sector. The mass scale is below 1 TeV and it is determined from below by the LHC searches and from above by the $(g-2)_\mu$ constraint.
- The preferred value for M_A is far in the decoupling limit. This is required by the fact that the observed properties of the (light) Higgs boson observed at the LHC are SM-like and by direct searches for heavy Higgs bosons.

The SLHA file corresponding to the best fit point can be downloaded from the `MasterCode` website [28].

3.2 Mass spectrum

In fig. 2 we plot the allowed 68% CL (dark peach) and 95% CL (light peach) intervals. In blue we also report the mass values of the best-fit point. From this plot we can observe that the masses for the colored sparticles (gluino and the squarks) and for the heavy Higgs are poorly constrained, since the LHC searches impose only a lower bound on them. On the other hand, the allowed mass range for electroweakinos and sleptons is much more restricted by the requirement of yielding the correct CDM relic density and by the measured value of $(g-2)_\mu$.

3.3 The muon anomalous magnetic dipole moment

The current measured value for $(g-2)_\mu$ deviates by $\sim 3.5\sigma$ [29] from the most precise SM prediction[30, 31]. However it possible to accommodate for the observed value in SUSY models. Indeed contributions from SUSY particles can be significant if smuons, charginos and the the lightest neutralinos have masses around 100 GeV. However, as we have already recalled, in

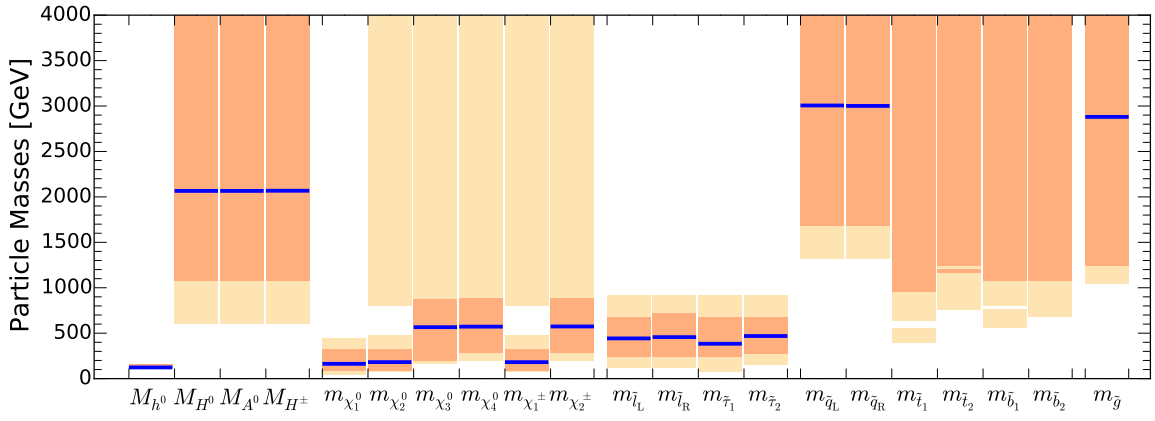

Figure 2: Mass ranges as predicted by our pMSSM10 fit. We show using dark (light) peach bars the 68% CL (95% CL) interval for the all the SUSY particles. The blue horizontal lines mark the values of the masses at the best-fit point.

SUSY GUT models, due to the implicit relation between colored and un-colored sparticle masses imposed by unification assumptions, the constraints coming from LHC searches and the observed Higgs mass on colored SUSY particles have the effect of preferring relatively heavy electroweak sparticle, therefore making difficult to explain the observed $(g-2)_\mu$ value with SUSY.

On the left of fig. 3, we show the $\Delta\chi^2$ from $(g-2)_\mu$ to the global χ^2 function in the pMSSM10 (black solid curve), and for comparison, in three GUT models that we analyzed in a series of previous papers (CMSSM, NUHM1,NUHM2). We also show the assumed experimental likelihood (red solid curve). We observe that indeed, differently from the GUT models, the pMSSM10 is perfectly able to reproduce the observed $(g-2)_\mu$ value, with $\Delta\chi^2 \sim 0$ in the case of the best fit point.

On the right of fig. 3, we plot the global χ^2 function of the $(g-2)_\mu$ with (solid black line) and without (dashed black line) the LHC electroweak constraints. We observe that they have little effect on the capability of the pMSSM10 to resolve the $(g-2)_\mu$ puzzle.

3.4 Perspectives for SUSY discovery

Now that the LHC has been restarted and it has been collecting new data, it is important to understand what are the prospects for SUSY discovery/exclusion, considering the parameters space that it is still allowed after the LHC Run 1.

3.4.1 SUSY Discovery after LHC Run 1

On the top left of fig. 4 we plot the 68% CL (red contours) and the 95% CL (blue contours) two-dimensional likelihood in the $(m_{\tilde{q}}, m_{\tilde{g}})$ plane[1] as well as the estimated 5σ discovery (95% CL_s exclusion) sensitivity with 300 fb^{-1}, using solid (dashed) magenta lines from ATLAS [32] via generic $\not{E}_T$ searches. We can see that the region of the parameter space preferred by our fit will be probed by the LHC in large part, including the best-fit point. Concerning the latter, nevertheless

[1] We use the symbol $m_{\tilde{q}}$ to denote the average of the masses of the first two generation squarks.

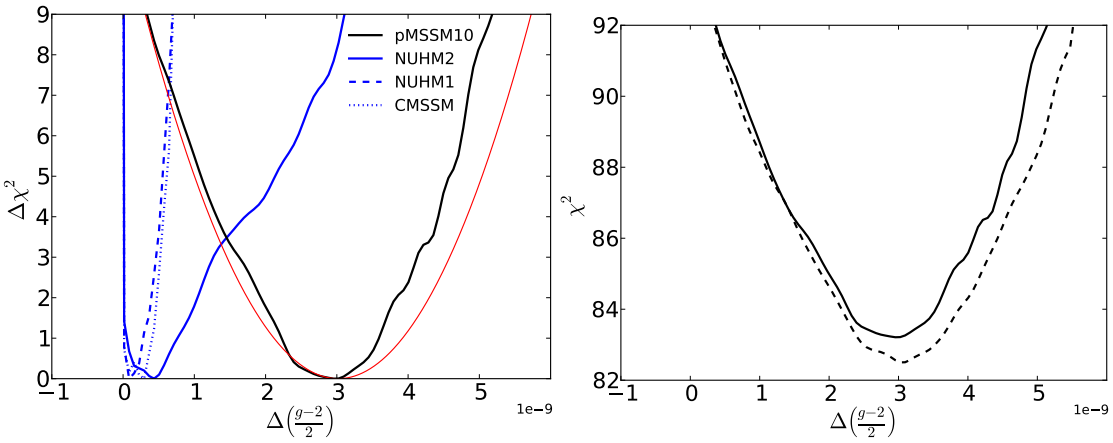

Figure 3: On the left: $\Delta\chi^2$ contribution of the $(g-2)_\mu$ constraint to the global fit for the CMSSM (dotted blue), NUHM1 (dashed blue), NUHM2 (solid blue) and the pMSSM10 (solid black). We also plot, as a reference, our assumed experimental likelihood using a solid red curve. On the right: global χ^2 curve, in the pMSSM10, with (solid black) and without (dashed black) the constraints coming from electroweakly-interacting sparticle searches at the LHC.

we have to recall that the masses of the colored sparticles are in general poorly determined and therefore also the position of the best fit point in the $(m_{\tilde{q}}, m_{\tilde{g}})$ plane.

In the top right pane of fig. 4, we plot again the two-dimensional likelihood contours, with the same color coding, in the $(m_{\tilde{t}_1}, m_{\tilde{\chi}_1^0})$ plane. The color shading represents the dominant decay channel (i.e. the one larger than 50%) in a specific point. We show using solid black lines the exclusion sensitivity for the $\tilde{t}_1 \to \tilde{\chi}_1^0 t$ decay mode [33]. We see that, with this channel only, the LHC will not be able to probe the compressed-stop region. However, it is possible to probe this section of the parameter space using the $\tilde{t}_1 \to \tilde{\chi}_1^\pm b$ decay channel. We show as a pale blue line the rescaled 95% CL_s limit contour, from the dibottom analysis, assuming that $m_{\tilde{\chi}_1^\pm} - m_{\tilde{\chi}_1^0} \sim 5$ GeV, obtained using the `Collider Reach` tool [34] for 300 fb^{-1}. We see that it would be able to probe part of the 95% CL compressed-stop region.

Next, we show on the bottom left of fig. 4 the $(m_{\tilde{\chi}_1^\pm}, m_{\tilde{\chi}_1^0})$ plane, with the 68% CL and the 95% CL contours shown again in red and blue respectively. Again, the color shadings reflect the dominant $\tilde{\chi}_1^\pm$ decay channel, with the color coding as specified in the legend. Using the same color scheme of the shadings, we show the sensitivity with 300 (3000) fb^{-1} [35] as solid (dashed) contours in the various decay channels. We see that with 300 fb^{-1} of data, the Wh search will cover almost all of the 95% CL region with low neutralino masses ($\lesssim 80$ GeV). To probe the remaining 95% CL region we have to rely on other final states (e.g. $\tilde{\chi}_1^\pm \to f\bar{f}'\,\tilde{\chi}_1^0/\tilde{\chi}_2^0 \to f\bar{f}\tilde{\chi}_1^0$).

Finally, we show in the bottom right panel the $(m_{\mu_R}, m_{\tilde{\chi}_1^0})$ plane. We show again, with the same color coding as before, the 68% CL (red) and the 95% CL (blue) contours. As before, we use the color shading to denote the dominant channel, in this case for the decay of the μ_R. We notice that the plane is dominated almost everywhere by the decay channel $\mu_R \to \mu\tilde{\chi}_1^0$. With a solid (dashed) pale blue line we show the sensitivity of the LHC with 300 fb^{-1} (3000 fb^{-1}), again obtained with the help of the `Collider Reach` tool. We observe that with 300 fb^{-1} the LHC would be able

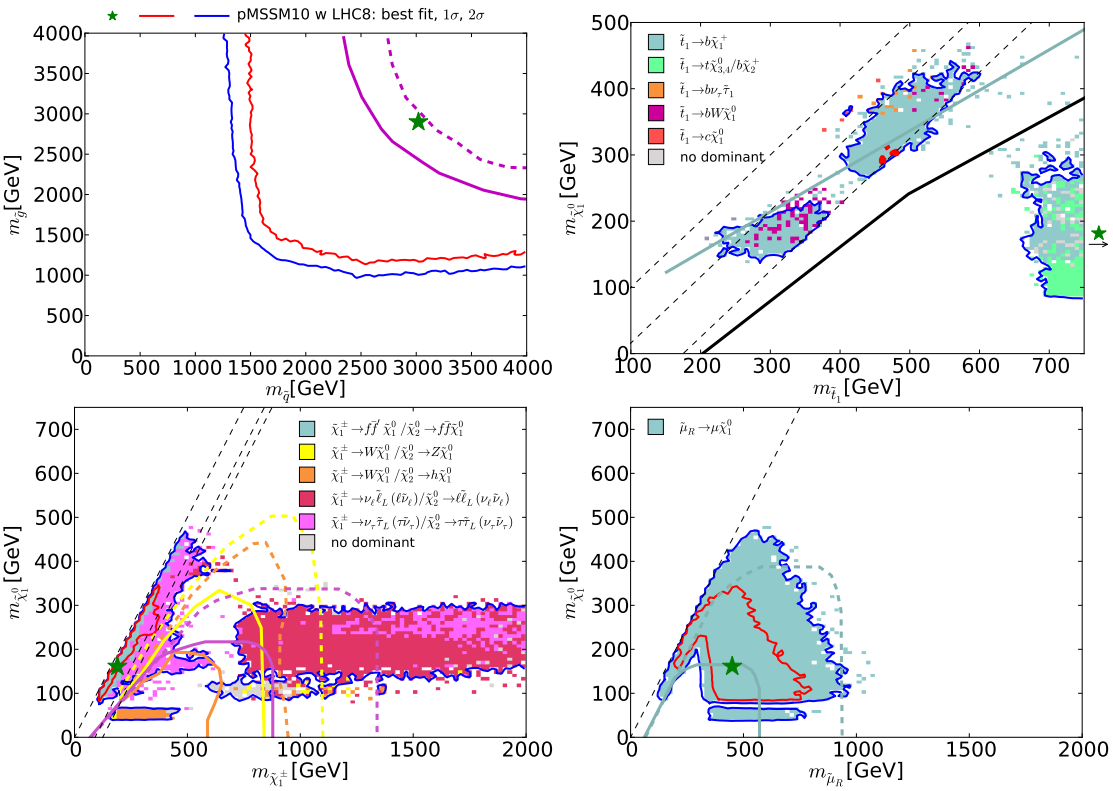

Figure 4: Bi-dimensional projections of our preferred pMSSM10 parameter space. For each location in the plane, we take the point in the full multi-dimensional parameter space with lowest global χ^2. The 68% CL and 95% CL contours are plotted in red and blue respectively. The best fit point is marked by a filled green star. In the upper left panel we show the results in the $(m_{\tilde{q}}, m_{\tilde{g}})$ plane. We plot with solid (dashed) purple lines the 5σ discovery (95% CL$_s$ exclusion) sensitivity with 300 fb^{-1} via generic $\not{E}_T$ searches from ATLAS. In the upper right plot, we show the results in the $(m_{\tilde{t}_1}, m_{\tilde{\chi}_1^0})$ plane. The sensitivity with an integrated luminosity of 300 fb^{-1} in the $\tilde{t} \to \tilde{\chi}_1^0 t$ ($\tilde{t}_1 \to \tilde{\chi}_1^\pm b$) decay channel is show with a thick black (pale blue) line. In the left right plot, we display the $(m_{\tilde{\chi}_1^\pm}, m_{\tilde{\chi}_1^0})$ plane. The shadings are used to indicate the dominant $\tilde{\chi}_1^\pm$ decay channel. The projected 95% CL$_s$ limits in the various channels with 300 fb^{-1} (3000 fb^{-1}) are show with a solid (dashed) line. In the bottom right panel, we plot the $(\mu_R, m_{\tilde{\chi}_1^0})$ plane, using again the shading to indicate the dominant decay channel and showing with solid (dashed) contours the 95% exclusion reach with 300 fb^{-1} (3000 fb^{-1})

to probe a large part of the 68% CL region and that it will explore most of the 95% CL region with 3000 fb^{-1}.

3.4.2 Discovery at e^+e^- colliders

In fig. 5 we show the one-dimensional likelihood curves for the lowest particle pair and associated chargino and neutralino production thresholds in e^+e^- collision, in the pMSSM10 (solid black) and in the CMSSM (dotted blue), NUHM1 (dashed blue) and NUHM2 (solid blue). We can see from the upper left, upper right and bottom right panels that the χ^2 minimum for $\tilde{\chi}_1^0\tilde{\chi}_1^0$, $\tilde{\chi}_1^0$ and $\tilde{\chi}_1^+\tilde{\chi}_1^-$ production respectively is within the reach of a e^+e^- collider with a center-of-mass energy $\sqrt{S}$ of 500 GeV. Moreover, a $\sqrt{S} = 1000$ GeV collider will be able to probe all thresholds inside

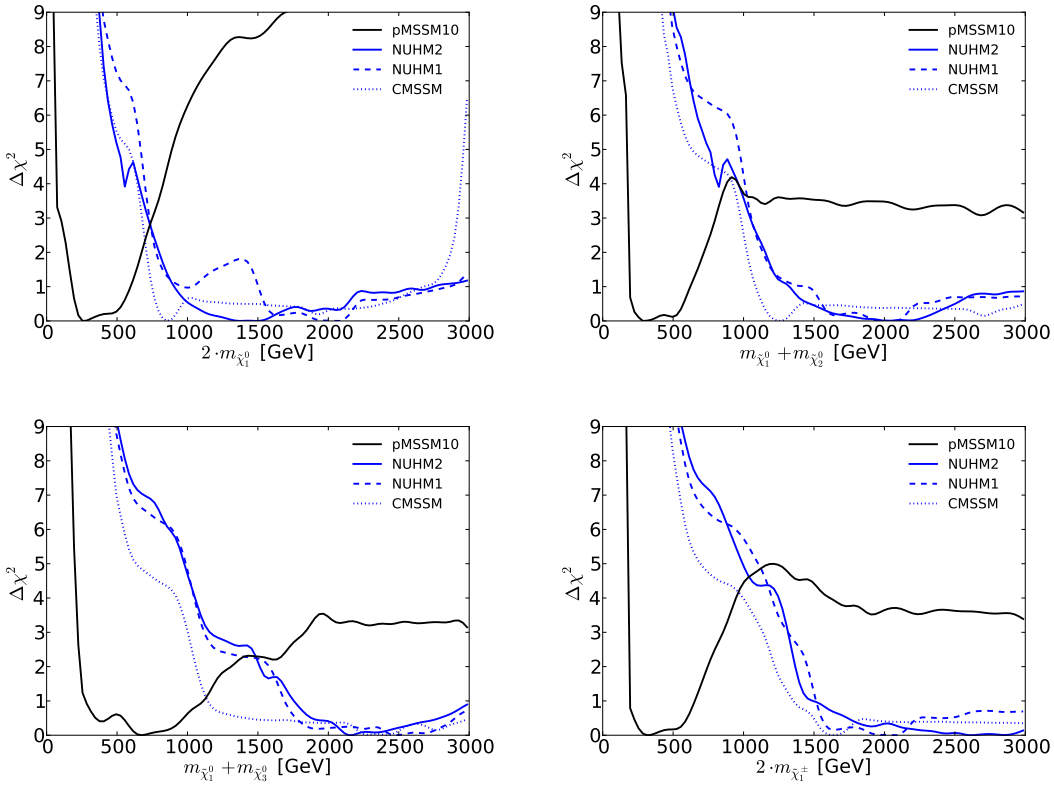

Figure 5: One dimensional likelihood profiles for various production thresholds at e^+e^- colliders, in the CMSSM (dotted blue), NUHM1 (dashed blue), NUHM2 (solid blue) and the pMSSM10 (solid black). We show $\chi_1^0\chi_1^0$ ($\tilde{\chi}_1^+\tilde{\chi}_1^-$) production in the top left (bottom right) plot and associated $\tilde{\chi}_1^0\tilde{\chi}_2^0$ ($\tilde{\chi}_1^0\tilde{\chi}_3^0$) production in the top right (bottom left) panel.

the $\Delta\chi^2 \leq 3$ interval. From the lower left plot, on the other hand, we observe that in the case of $\tilde{\chi}_1^0\tilde{\chi}_3^0$, the global χ^2 minimum lies around 600 GeV. It is interesting to note that the pMSSM10 has much lower thresholds compared with the GUT models, with the latter requiring higher $\sqrt{S}$ values to be effectively explored at a e^+e^- collider.

4. Conclusions

In this proceeding we have briefly presented some of the results of our recent paper [1] where we have performed the first global frequentist likelihood analysis of the pMSSM10, including a treatment of the LHC constraints from Run 1 searches. To achieve this goal we have extended the `MasterCode` framework to allow for a consistent inclusion of the LHC searches. We have found that the masses of colored sparticles are poorly constrained, since experimental searches provide only a lower bound on their values. On the other hand, the masses of the electroweakinos and of the sleptons are much better determined due to the constraints coming from $(g-2)_\mu$ and the CDM relic density. Indeed one of the most interesting results that we have found is the possibility in the pMSSM10 (differently from the GUT models) of accommodating for the observed value of $(g-2)_\mu$ while at the same time respecting all the constraints coming from the available LHC data.

Concerning the perspective of SUSY discovery, we have found that LHC at 14 TeV will have the possibility of probing large part of the preferred regions of $m_{\tilde{q}}$ and $m_{\tilde{g}}$ and a significant portion of the parameter space for light $\tilde{t}_1$ and $\tilde{\mu}$. We have also found that our preferred region will be within the reach of a collider with center-of-mass energy between 500 GeV and 1000 GeV. We refer to ref. [1] for a more complete description of our results.

References

[1] K. J. de Vries *et al.*, Eur. Phys. J. C **75** (2015) 9, 422 [arXiv:1504.03260 [hep-ph]].

[2] G. Aad *et al.* [ATLAS Collaboration], arXiv:1405.7875 [hep-ex];
full ATLAS Run 1 results can be found at
`https://twiki.cern.ch/twiki/bin/view/AtlasPublic/SupersymmetryPublicResults`.

[3] S. Chatrchyan *et al.* [CMS Collaboration], JHEP **1406** (2014) 055 [arXiv:1402.4770 [hep-ex]];
full CMS Run 1 results can be found at
`https://twiki.cern.ch/twiki/bin/view/CMSPublic/PhysicsResultsSUS`.

[4] M. Drees and M. M. Nojiri, Phys. Rev. D **47** (1993) 376 [arXiv:hep-ph/9207234]; H. Baer and M. Brhlik, Phys. Rev. D **53** (1996) 597 [arXiv:hep-ph/9508321]; Phys. Rev. D **57** (1998) 567 [arXiv:hep-ph/9706509]; H. Baer, M. Brhlik, M. A. Diaz, J. Ferrandis, P. Mercadante, P. Quintana and X. Tata, Phys. Rev. D **63** (2001) 015007 [arXiv:hep-ph/0005027]; J. R. Ellis, T. Falk, G. Ganis, K. A. Olive and M. Srednicki, Phys. Lett. B **510** (2001) 236 [hep-ph/0102098].

[5] G. L. Kane, C. F. Kolda, L. Roszkowski and J. D. Wells, Phys. Rev. D **49** (1994) 6173 [arXiv:hep-ph/9312272]; J. R. Ellis, T. Falk, K. A. Olive and M. Schmitt, Phys. Lett. B **388** (1996) 97 [arXiv:hep-ph/9607292]; Phys. Lett. B **413** (1997) 355 [arXiv:hep-ph/9705444]; J. R. Ellis, T. Falk, G. Ganis, K. A. Olive and M. Schmitt, Phys. Rev. D **58** (1998) 095002 [arXiv:hep-ph/9801445]; V. D. Barger and C. Kao, Phys. Rev. D **57** (1998) 3131 [arXiv:hep-ph/9704403]; J. R. Ellis, T. Falk, G. Ganis and K. A. Olive, Phys. Rev. D **62** (2000) 075010 [arXiv:hep-ph/0004169]; L. Roszkowski, R. Ruiz de Austri and T. Nihei, JHEP **0108** (2001) 024 [arXiv:hep-ph/0106334]; A. Djouadi, M. Drees and J. L. Kneur, JHEP **0108** (2001) 055 [arXiv:hep-ph/0107316]; U. Chattopadhyay, A. Corsetti and P. Nath, Phys. Rev. D **66** (2002) 035003 [arXiv:hep-ph/0201001]; J. R. Ellis, K. A. Olive and Y. Santoso, New Jour. Phys. **4** (2002) 32 [arXiv:hep-ph/0202110]; H. Baer, C. Balazs, A. Belyaev, J. K. Mizukoshi, X. Tata and Y. Wang, JHEP **0207** (2002) 050 [arXiv:hep-ph/0205325]; R. Arnowitt and B. Dutta, arXiv:hep-ph/0211417.

[6] S. S. AbdusSalam, *et al.*, Eur. Phys. J. C **71** (2011) 1835 [arXiv:1109.3859 [hep-ph]].

[7] H. Baer, A. Mustafayev, S. Profumo, A. Belyaev and X. Tata, Phys. Rev. D **71** (2005) 095008 [arXiv:hep-ph/0412059]; H. Baer, A. Mustafayev, S. Profumo, A. Belyaev and X. Tata, *JHEP* **0507** (2005) 065, hep-ph/0504001; J. R. Ellis, K. A. Olive and P. Sandick, Phys. Rev. D **78** (2008) 075012 [arXiv:0805.2343 [hep-ph]]; J. Ellis, F. Luo, K. A. Olive and P. Sandick, Eur. Phys. J. C **73** (2013) 2403 [arXiv:1212.4476 [hep-ph]].

[8] J. Ellis, K. Olive and Y. Santoso, Phys. Lett. B **539** (2002) 107 [arXiv:hep-ph/0204192]; J. R. Ellis, T. Falk, K. A. Olive and Y. Santoso, Nucl. Phys. B **652** (2003) 259 [arXiv:hep-ph/0210205].

[9] See, for example, C. F. Berger, J. S. Gainer, J. L. Hewett and T. G. Rizzo, JHEP **0902**, 023 (2009) [arXiv:0812.0980 [hep-ph]]; S. S. AbdusSalam, B. C. Allanach, F. Quevedo, F. Feroz and M. Hobson,

Phys. Rev. D **81**, 095012 (2010) [arXiv:0904.2548 [hep-ph]]; J. A. Conley, J. S. Gainer, J. L. Hewett, M. P. Le and T. G. Rizzo, Eur. Phys. J. C **71**, 1697 (2011) [arXiv:1009.2539 [hep-ph]]; J. A. Conley, J. S. Gainer, J. L. Hewett, M. P. Le and T. G. Rizzo, [arXiv:1103.1697 [hep-ph]]; B. C. Allanach, A. J. Barr, A. Dafinca and C. Gwenlan, JHEP **1107**, 104 (2011) [arXiv:1105.1024 [hep-ph]]; S. Sekmen, S. Kraml, J. Lykken, F. Moortgat, S. Padhi, L. Pape, M. Pierini and H. B. Prosper *et al.*, JHEP **1202** (2012) 075 [arXiv:1109.5119 [hep-ph]]; A. Arbey, M. Battaglia and F. Mahmoudi, Eur. Phys. J. C **72** (2012) 1847 [arXiv:1110.3726 [hep-ph]]; A. Arbey, M. Battaglia, A. Djouadi and F. Mahmoudi, Phys. Lett. B **720** (2013) 153 [arXiv:1211.4004 [hep-ph]]; M. W. Cahill-Rowley, J. L. Hewett, A. Ismail and T. G. Rizzo, Phys. Rev. D **88** (2013) 3, 035002 [arXiv:1211.1981 [hep-ph]]; C. Strege, G. Bertone, G. J. Besjes, S. Caron, R. Ruiz de Austri, A. Strubig and R. Trotta, JHEP **1409** (2014) 081 [arXiv:1405.0622 [hep-ph]]; M. Cahill-Rowley, J. L. Hewett, A. Ismail and T. G. Rizzo, Phys. Rev. D **91** (2015) 5, 055002 [arXiv:1407.4130 [hep-ph]]; L. Roszkowski, E. M. Sessolo and A. J. Williams, JHEP **1502**, 014 (2015) [arXiv:1411.5214 [hep-ph]]; M. E. C. Catalan, S. Ando, C. Weniger and F. Zandanel, arXiv:1503.00599 [hep-ph]; J. Chakrabortty, A. Choudhury and S. Mondal, arXiv:1503.08703 [hep-ph].

[10] P. Skands *et al.*, JHEP **0407** (2004) 036 [arXiv:hep-ph/0311123]; B. Allanach *et al.*, Comput. Phys. Commun. **180** (2009) 8 [arXiv:0801.0045 [hep-ph]].

[11] F. Feroz and M. P. Hobson, Mon. Not. Roy. Astron. Soc. **384**, 449 (2008) [arXiv:0704.3704 [astro-ph]].

[12] F. Feroz, M. P. Hobson and M. Bridges, Mon. Not. Roy. Astron. Soc. **398** (2009) 1601 [arXiv:0809.3437 [astro-ph]].

[13] F. Feroz, M. P. Hobson, E. Cameron and A. N. Pettitt, arXiv:1306.2144 [astro-ph.IM].

[14] O. Buchmueller and J. Marrouche, Int. J. Mod. Phys. A **29** (2014) 1450032 [arXiv:1304.2185 [hep-ph]].

[15] M. Papucci, K. Sakurai, A. Weiler and L. Zeune, `Atom`*: Automated Tests of Models*, *in preparation*.

[16] `Scorpion` was first developed by J. Marrouche, and developed further by O. Buchmueller, M. Citron, S. Malik and K.J. de Vries: details may be obtained by contacting O. Buchmueller.

[17] S. Heinemeyer *et al.*, JHEP **0608** (2006) 052 [arXiv:hep-ph/0604147]; S. Heinemeyer, W. Hollik, A. M. Weber and G. Weiglein, JHEP **0804** (2008) 039 [arXiv:0710.2972 [hep-ph]].

[18] G. Isidori and P. Paradisi, Phys. Lett. B **639** (2006) 499 [arXiv:hep-ph/0605012]; G. Isidori, F. Mescia, P. Paradisi and D. Temes, Phys. Rev. D **75** (2007) 115019 [arXiv:hep-ph/0703035], and references therein.

[19] F. Mahmoudi, Comput. Phys. Commun. **178** (2008) 745 [arXiv:0710.2067 [hep-ph]]; Comput. Phys. Commun. **180** (2009) 1579 [arXiv:0808.3144 [hep-ph]]; D. Eriksson, F. Mahmoudi and O. Stal, JHEP **0811** (2008) 035 [arXiv:0808.3551 [hep-ph]].

[20] Information about this code is available from K. A. Olive: it contains important contributions from T. Falk, A. Ferstl, G. Ganis, A. Mustafayev, J. McDonald, F. Luo, K. A. Olive, P. Sandick, Y. Santoso, V. Spanos, and M. Srednicki.

[21] G. Belanger, F. Boudjema, A. Pukhov and A. Semenov, Comput. Phys. Commun. **176** (2007) 367 [arXiv:hep-ph/0607059]; Comput. Phys. Commun. **149** (2002) 103 [arXiv:hep-ph/0112278]; Comput. Phys. Commun. **174** (2006) 577 [arXiv:hep-ph/0405253].

[22] G. Degrassi, S. Heinemeyer, W. Hollik, P. Slavich and G. Weiglein, Eur. Phys. J. C **28** (2003) 133 [arXiv:hep-ph/0212020]; S. Heinemeyer, W. Hollik and G. Weiglein, Eur. Phys. J. C **9** (1999) 343 [arXiv:hep-ph/9812472]; S. Heinemeyer, W. Hollik and G. Weiglein, Comput. Phys. Commun. **124** (2000) 76 [arXiv:hep-ph/9812320]; M. Frank *et al.*, JHEP **0702** (2007) 047 [arXiv:hep-ph/0611326]; See `http://www.feynhiggs.de` .

[23] T. Hahn, S. Heinemeyer, W. Hollik, H. Rzehak and G. Weiglein, Phys. Rev. Lett. **112** (2014) 141801 [arXiv:1312.4937 [hep-ph]].

[24] P. Bechtle, S. Heinemeyer, O. Stål, T. Stefaniak and G. Weiglein, Eur. Phys. J. C **74** (2014) 2, 2711 [arXiv:1305.1933 [hep-ph]]; JHEP **1411** (2014) 039 [arXiv:1403.1582 [hep-ph]].

[25] P. Bechtle, O. Brein, S. Heinemeyer, G. Weiglein and K. E. Williams, Comput. Phys. Commun. **181** (2010) 138 [arXiv:0811.4169 [hep-ph]], Comput. Phys. Commun. **182** (2011) 2605 [arXiv:1102.1898 [hep-ph]]; P. Bechtle *et al.*, Eur. Phys. J. C **74** (2014) 3, 2693 [arXiv:1311.0055 [hep-ph]].

[26] B. C. Allanach, G Comput. Phys. Commun. **143** (2002) 305 [arXiv:hep-ph/0104145].

[27] M. Muhlleitner, A. Djouadi, Y. Mambrini, Comput. Phys. Commun. **168** (2005) 46 [arXiv:hep-ph/0311167].

[28] `MasterCode` home page, http://mastercode.web.cern.ch/

[29] G. Bennett et al. [The Muon g-2 Collaboration], *Phys. Rev. Lett.* **92** (2004) 161802, [arXiv:hep-ex/0401008]; and *Phys. Rev.* **D 73** (2006) 072003 [arXiv:hep-ex/0602035].

[30] D. Stockinger, J. Phys. G **34** (2007) R45 [arXiv:hep-ph/0609168]; J. Miller, E. de Rafael and B. Roberts, *Rept. Prog. Phys.* **70** (2007) 795 [arXiv:hep-ph/0703049]; J. Prades, E. de Rafael and A. Vainshtein, arXiv:0901.0306 [hep-ph]; F. Jegerlehner and A. Nyffeler, Phys. Rept. **477**, 1 (2009) [arXiv:0902.3360 [hep-ph]]; M. Davier, A. Hoecker, B. Malaescu, C. Z. Yuan and Z. Zhang, Eur. Phys. J. C **66**, 1 (2010) [arXiv:0908.4300 [hep-ph]]. J. Prades, Acta Phys. Polon. Supp. **3**, 75 (2010) [arXiv:0909.2546 [hep-ph]]; T. Teubner, K. Hagiwara, R. Liao, A. D. Martin and D. Nomura, arXiv:1001.5401 [hep-ph]; M. Davier, A. Hoecker, B. Malaescu and Z. Zhang, Eur. Phys. J. C **71** (2011) 1515 [arXiv:1010.4180 [hep-ph]].

[31] F. Jegerlehner and R. Szafron, Eur. Phys. J. C **71** (2011) 1632 [arXiv:1101.2872 [hep-ph]]; M. Benayoun, P. David, L. DelBuono and F. Jegerlehner, Eur. Phys. J. C **73** (2013) 2453 [arXiv:1210.7184 [hep-ph]].

[32] ATLAS Collaboration, arXiv:1307.7292 [hep-ex]

[33] ATLAS Collaboration, ATL-PHYS-PUB-2013-011.

[34] G. Salam and A. Weiler, http://collider-reach.web.cern.ch/

[35] ATLAS Collaboration, ATL-PHYS-PUB-2014-010.